Optical third-harmonic studies of the dispersion in $\bar{\chi}^{(3)}$ for gallium nitride thin films on sapphire

J. Miragliotta* and D. K. Wickenden
Applied Physics Laboratory, The Johns Hopkins University, Johns Hopkins Road, Laurel, Maryland 20723-6099
(Received 16 March 1994)

Third-harmonic (TH) transmission spectroscopy was used to study the dispersion in the $\chi^{(3)}_{xxxx}$ element of the third-order susceptibility in wurtzite-phase gallium nitride (GaN) films on sapphire. Analysis of the nonlinear response showed an enhancement in $\chi^{(3)}_{xxxx}$ when the photon energy of the TH field was tuned to the absorption edge, $E_g = 3.398$ eV, with a peak value of 2.7×10^{-11} e.s.u. Comparison with previous band-structure calculations of $\chi^{(3)}_{xxxx}$ in wide-band-gap zinc-blende semiconductors shows that the dispersion in GaN is qualitatively similar to the third-order response in ZnSe near the absorption edge.

I. INTRODUCTION

Integrated-optical devices using nonlinear materials offer the potential for advancements in technologically important applications such as optical mixing and modulation, signal processing and computing, and optoelectronics. Success in these fields, however, is dependent on the development of novel materials that possess relatively large second- and third-order nonlinear susceptibilities [$\bar{\chi}^{(2)}$ and $\bar{\chi}^{(3)}$, respectively] and can be conveniently deposited as homogeneous thin films for optical waveguide structures. Although experimental research regarding the nonlinear optical response in thin films has primarily focused on π-conjugated organic compounds and ferroelectric inorganic crystals such as $LiNbO_3$,[1,2] recent band-structure calculations of wide-band-gap zinc-blende II-VI and III-V semiconductors have predicted $\bar{\chi}^{(2)}$ and $\bar{\chi}^{(3)}$ magnitudes that are comparable to these more conventional systems.[3-7] To date, however, there has been little experimental support of the third-order nonlinear theoretical results.[8,9]

A tetrahedrally coordinated III-V compound that has received considerable attention over the past decade is gallium nitride (GaN), a wide-band-gap semiconductor that can be epitaxially deposited as a homogeneous thin film in either a hexagonal wurtzite or cubic zinc-blende crystal phase.[10] Activity regarding the material characterization of this metal nitride is due to the direct band gap ($E_g \sim 3.4$ eV for the wurtzite phase) in undoped GaN, which can be tailored for the production of tunable electro-optic devices in the UV and visible wavelength range of the spectrum, particularly when alloyed with either AlN or InN. Although a handful of band-structure calculations regarding the linear optical response of the wurtzite phase have been performed,[11,12] analogous theoretical studies of the second- and third-order nonlinearities in GaN have not been reported. In fact, experimental investigations of $\bar{\chi}^{(2)}$ in GaN have relied on bonding-molecular-orbital calculations for interpretation,[13,14] models which do not include dispersion effects.

In this paper, the experimental results obtained by optical third-harmonic (TH) generation spectroscopy for the dispersion and magnitude of the $\chi^{(3)}_{xxxx}$ element in the third-order susceptibility in wurtzite-phase GaN are presented. A resonant enhancement was observed in $\chi^{(3)}_{xxxx}$ near the direct fundamental energy gap of GaN (E_0 critical point), with a peak magnitude that exceeded 10^{-11} esu in this photon energy range. Comparison with previous band-structure calculations of $\chi^{(3)}_{xxxx}$ in wide-band-gap cubic zinc-blende semiconductors [Ghahramani, Moss, and Sipe[4] (GMS) and Ching and Huang[7] (CH)] show a strong correlation between the dispersion in GaN and the predicted third-order response in ZnSe for TH photon energies near the absorption edge. This result was attributed to the similarities in the electronic structure of these respective materials at the E_0 critical point of the band structure.

II. EXPERIMENT

The details concerning the deposition of high-quality, crystalline GaN epitaxial films on sapphire have been discussed in detail elsewhere.[15] The GaN films were grown in a vertical spinning-disc metal-organic chemical-vapor deposition (MOCVD) reactor using trimethyl gallium and ammonia gases as the source materials. The intrinsically undoped epitaxial films were oriented with the c axis (optical axis) of the GaN crystal parallel to the (0001) axis of the substrate and normal to the sample surface. In addition, a 30° azimuthal rotation of the GaN layer with respect to the underlying sapphire substrate oriented the $(10\bar{1}0)$ of the film parallel to the $(11\bar{2}0)$ of the substrate.

TH investigations were performed by measuring the TH signal from a GaN/sapphire in air sample as a function of the incident (ω) photon energy. Due to the ambient nature of the experiment, the transmitted TH intensity nonlinear was measured rather than the reflected signal, so as to minimize the effects of surface contamination and oxidation. Stimulated Stokes Raman scattering of tunable dye laser radiation (1.52–1.87 eV) in a high-pressure volume of H_2 gas (10 atm, 2-m beam path) produced the high peak power, fundamental light source in the 1.00–1.35-eV photon energy range. The laser radiation was linearly polarized and normally incident at the

air/GaN interface of the sample, with a power density of ~ 1 MW/cm^2. The TH nature of the detected signal was verified by demonstrating its cubic dependence to the incident IR intensity. The sample signal was normalized to the corresponding TH intensity from a separate sapphire substrate which has minimal dispersion in this photon energy range. We note that the incident laser source was spectrally filtered of any TH signal that was generated in the incident optics or air. Also, the third-order nonlinearity of sapphire [$\chi^{(3)}_{xxxx}=1.15\times10^{-14}$ esu (Ref. 16)] did not produce a detectable TH signal relative to the GaN thin film.

III. THEORY

TH as a technique for the characterization of $\bar{\chi}^{(3)}$ has been previously described elsewhere.[9,17] Similar to second-harmonic generation, the coupling efficiency between the incident laser source and $\bar{\chi}^{(3)}$ is dependent on the symmetry of the material and the propagation direction and polarization of fundamental light source (ω). In hexagonal GaN, which has a 6-mm point-group symmetry, there are four independent elements to this fourth rank tensor:[18] $\chi^{(3)}_{zzzz}$, $\chi^{(3)}_{xxxx}$, $\chi^{(3)}_{xxzz}$, and $\chi^{(3)}_{zzxx}$. Under the conditions of normal incidence, coupling between the incident fundamental beam and the third-order nonlinearity can only occur through the $\chi^{(3)}_{xxxx}$ element, since the direction of the optical axis in the GaN thin film (z axis of the crystal) is parallel to the surface normal of the sample. The direction of the film optical axis coupled with the high refractive index of GaN at ω ($n\sim2.4$) prevented efficient coupling to the z-dependent elements in $\bar{\chi}^{(3)}$.

The third-harmonic polarization induced in the GaN sample under normal incidence is

$$P^{(3)}_y(3\omega,z)=\chi^{(3)}_{xxxx}(-3\omega;\omega,\omega,\omega)E^3_y(\omega,z)\ , \tag{1}$$

where the fundamental field in the film, $E_y(\omega,z)$, is directed along the y axis of the crystal, the xy plane of the crystal is aligned with the surface plane GaN, and z is in the direction of the surface normal. To determine the magnitude and dispersion of $\chi^{(3)}_{xxxx}$, tractable solutions to the nonlinear electromagnetic response of a thin dielectric film at frequency 3ω to an incident source of frequency ω were deduced from the usual boundary conditions for the fields at the plane interfaces between the nonlinear and linear media.[9,13] Multiple reflections at the two GaN interfaces were included in the electromagnetic model since both linear and nonlinear transmission spectra suggested their importance (see Fig. 1). For an ω light source incident at the air/GaN interface, the TH signal transmitted through the sapphire/air interface is

$$I_{3\omega}=\frac{c(f_1^*f_1)|\chi^{(3)}_{xxxx}|^2}{8\pi}\ , \tag{2}$$

with

$$f_1=\frac{4\pi f_2 T_{31}}{n^2_\omega-n^2_{3\omega}}\ , \tag{3}$$

where the wavelength notation on $\chi^{(3)}_{xxxx}$ has been omitted, and c is the speed of light. The function f_2 is given by

$$f_2=\frac{f_3\exp(i\phi_f)(1+R_{23})}{1+R_{12}R_{23}\exp(2i\phi_f)}+f_4\ , \tag{4a}$$

with

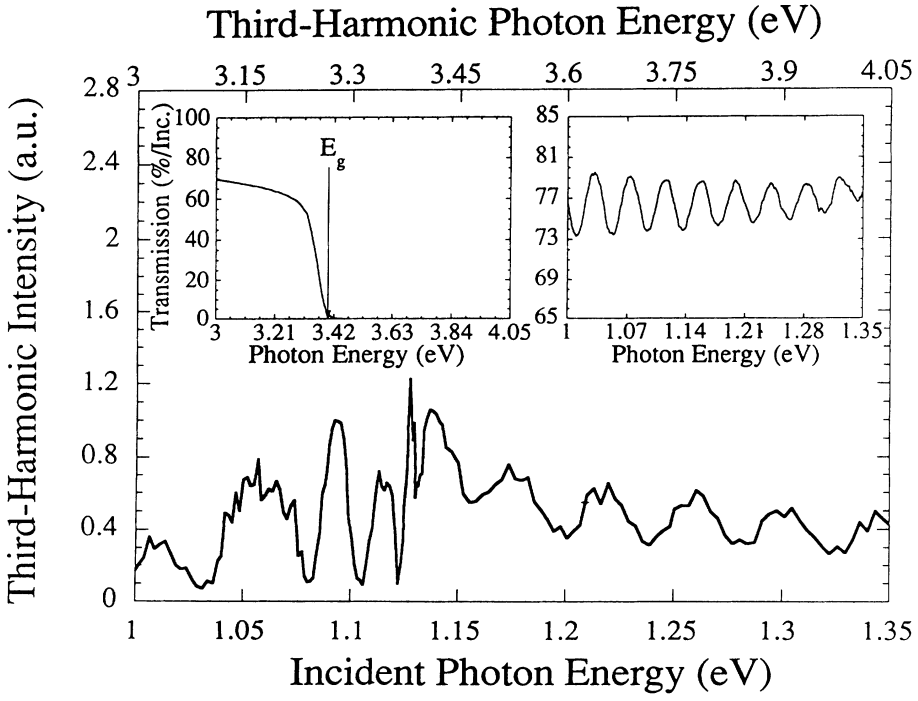

FIG. 1. The third-harmonic intensity in arbitrary units from a 6.08-μm GaN film on sapphire as a function of the photon energy of the incident laser source. The left and right insets, respectively, are the normal incidence linear transmission spectra in the third-harmonic (3ω) and fundamental (ω) photon energy regions. The vertical arrow in the left inset denotes the position of the band edge.

$$f_3 = \frac{E_y^3(\omega,d)\left[1-\frac{n_\omega}{n_T}\right]R_{12}\exp(i\phi_f)}{\left[1+\frac{n_{3\omega}}{n_T}\right]} - \frac{E_y^3(\omega,0)(1+n_\omega)}{(1+n_{3\omega})} \quad (4b)$$

and

$$f_4 = \frac{E_y^3(\omega,d)(n_{3\omega}+n_\omega)}{(n_T+n_{3\omega})} . \quad (4c)$$

In these expressions, $n_{\omega(3\omega)}$ is the refractive index of the GaN film at the fundamental (third-harmonic) frequency, and n_T is the refractive index of the sapphire substrate at 3ω.[19] R_{12}, R_{23}, and T_{31} are the Fresnel coefficients which account for reflection (3ω) at the air/GaN and GaN/sapphire interfaces and transmission across the sapphire/air interface. $E_y(\omega,0(d))$ is the fundamental field at the front (back) surface of the film which contains the phase factors associated with propagation in the film. ϕ_f is the optical phase of the third-harmonic field at the GaN/sapphire interface. The refractive index at ω and 3ω was characterized by the ordinary value of the refractive index, since the optical fields and induced polarization vectors were oriented perpendicular to the optical axis.

IV. RESULTS AND DISCUSSION

Figure 1 shows the TH transmitted intensity from a 6.08-μm-thick film in the ω (3ω) photon energy range of 1.00–1.35 eV (3.00–4.05 eV). The left inset shows the linear transmission (ω) scan in the band-gap region which determined the fundamental absorption energy ($E_g = 3.398$ eV) and verified the direct nature of the E_0 optical transition. For 3ω energies below E_g, the TH transmitted signal exhibited a rapid oscillatory behavior which was attributed to the wavelength dependence of the phase velocity mismatch between the free and bound third-harmonic waves.[20] The period associated with maximum interference between the third-harmonic waves, i.e., the energy separation between TH minimum intensity, was observed to increase with decreasing photon energy due to the increase in the nonlinear optical coherence length of the GaN film. These oscillations terminated for 3ω photon energies $> E_g$ due to the strong absorption of the TH field in the film. In this photon energy range, the signal variations were due to the multibeam interference of the fundamental beam in the thin film (see right inset of Fig. 1).

Examination of Eqs. (2)–(4) show that the photon energy dependence and absolute magnitude of $\chi^{(3)}_{xxxx}$ can be determined from the detected TH signal if the values for the film thickness, d and $n_{\omega(3\omega)}$ are known parameters. Linear reflectance and transmission measurements were used to determine the film thickness and the refractive indices in the transparent region of the material ($3\hbar\omega < 3.2$ eV). For 3ω photon energies near and above the fundamental absorption edge ($3\hbar\omega > 3.2$ eV), values for the real and imaginary parts of $n_{3\omega}$ were taken from the literature.[21] The square root of the TH signal in Fig. 1 was normalized to the product of the scale factor f_1 and $(c/8\pi)^{1/2}$, generating the experimentally derived spectrum of $\chi^{(3)}_{xxxx}$. Figure 2 shows the results of this normalization procedure and the f_1 spectrum which is enhanced for 3ω photon energies below the absorption edge in GaN (inset of Fig. 1). The $\chi^{(3)}_{xxxx}$ spectrum exhibited a resonant enhancement for 3ω photon energies near the absorption edge, peaking at 2.7×10^{-11} esu with a monotonic de-

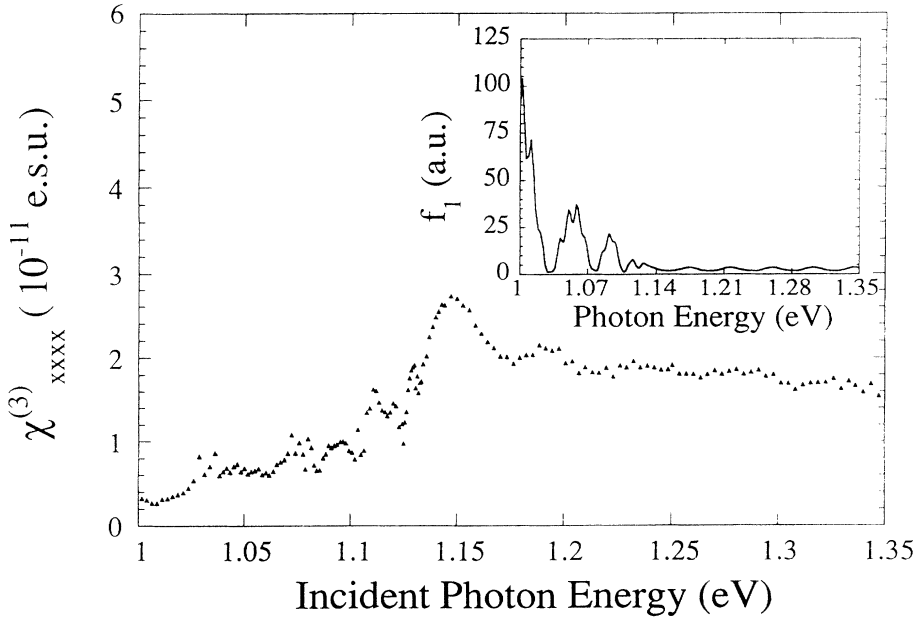

FIG. 2. The magnitude of $\chi^{(3)}_{xxxx}$ in GaN as a function of the photon energy of the incident laser source. The inset is a graphical representation of the function f_1 in Eq. (2).

crease in value with increasing energies. Under the room-temperature conditions of this investigation, there was no observation of valence-band splitting near the band edge or additional resonances in the spectrum, e.g., the E_1 critical point transition or band-edge excitonic effects.

Recently, band-structure calculations of $\chi^{(3)}_{xxxx}$ by GMS and CH have determined the dispersion and magnitude of the third-order susceptibility for a collection of cubic zinc-blende III-V and II-VI semiconductors. In these investigations, which were based on either empirical tight-binding and *semi-ab initio* (GMS) or self-consistent approaches (CH), low-energy critical points in the joint density of states (E_0 and E_1) were more noticeable in the third-order nonlinear response as compared to the linear or second-order susceptibilities. Additionally, the third-order susceptibility for a general crystal structure, e.g., wurtzite or zinc blende, was shown to have a E^7_ω photon energy dependence with contributions from ω (fundamental), 2ω, and 3ω (TH) resonances at the E_0 and E_1 critical points. Specifically, the dispersion of $\chi^{(3)}_{xxxx}$ in wide-band-gap materials such as ZnS and ZnSe was shown to be dominated by direct three-state resonances with the direct fundamental absorption edge (E_0) and the E_1 critical points, with smaller contributions from 3ω virtual-hole or -electron transitions or higher-energy 2ω resonances. As is evident from the data in Fig. 2, the single resonance at the fundamental absorption edge and subsequent decrease in $\chi^{(3)}_{xxxx}$ for increasing 3ω photon energies is qualitatively similar to the predicted behavior in these earlier calculations. The dispersion in GaN, where the energy separation between the E_0 and E_1 critical points is ~ 4 eV,[11,12] is clearly dominated by the 3ω resonance at the absorption edge with little contribution from either the 2ω resonance with this transition ($\omega = 1.7$ eV) or 3ω resonances with higher interband transitions ($E_1 \sim 7.2$ eV).

Despite the inability to compare the experimental results of Fig. 2 with a wurtzite band-structure calculation of $\chi^{(3)}_{xxxx}$ directly, the similarities in the electronic properties of hexagonal and zinc-blende phase GaN (Refs. 11 and 12) should allow a reasonable comparison to the nonlinear zinc-blende calculations of GMS and CH. In the wurtzite phase, the hexagonal crystal field induces a splitting in the valence bands at the Brillouin-zone center (Γ) which lifts the degeneracy associated with the E_0 critical point and creates an optical anisotropy that is not present in the cubic structure. However, low-temperature optical investigations and band-structure calculations of GaN have shown that the valence-band splitting at the absorption edge point does not exceed 0.02 eV (Ref. 22) due to the relatively small lattice constant of the material ($a_{GaN} = 3.189$ A). This degree of splitting is not observable in room-temperature investigations, and assures that the critical points in the joint density of states of hexagonal and cubic GaN are very similar.[12] In fact, absorption measurements near the E_0 critical point have shown that the band-edge excitation is direct in both systems, with a band-gap energy difference of ~ 0.2 eV. In Fig. 3, the experimental $\chi^{(3)}_{xxxx}$ spectrum of GaN is plotted with the

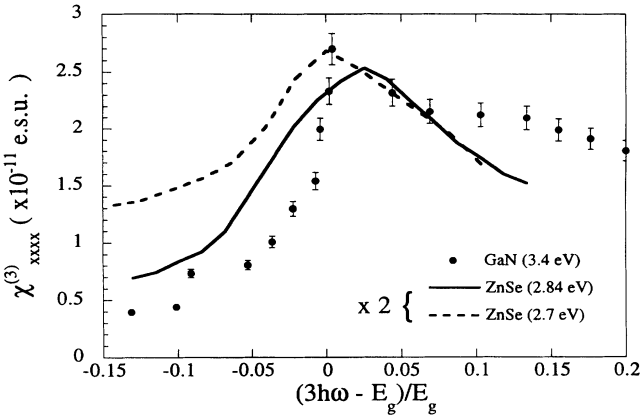

FIG. 3. Comparison of the experimental value of $\chi^{(3)}_{xxxx}$ in GaN with the theoretical prediction of this nonlinearity in zinc-blende ZnSe. The calculated spectra from Refs. 4 (solid line) and 7 (dashed line) are scaled by a factor of 2 with respect to the GaN data. The $\chi^{(3)}_{xxxx}$ values are plotted against the normalized (E_g) difference between the 3ω photon and band-edge energies (energy values in parentheses).

corresponding nonlinearity in ZnSe as calculated by GMS (solid line) and CH (dashed line). In this plot, the $\chi^{(3)}_{xxxx}$ spectra have been plotted as a function of the energy difference between the 3ω photon and E_g, normalized to E_g of the respective material. The ZnSe data were obtained by digitizing the theoretical results from CH and GMS. ZnSe was chosen for the comparison since, like GaN, it has direct valence-to-conduction-band transitions at the fundamental absorption edge [($E_g = 2.84$ eV) (Ref. 4)]. Also, the density of states in ZnSe and GaN have upper valence-band states that are dominated by the p orbitals of the anion (Se or N), and a lower conduction-band region dominated by the s orbitals of the cation (Zn or Ga). As such, the critical points in the joint density of states are very similar in these two materials,[23] provided the effect of spin-orbit coupling at the band edge is neglected in the II-VI semiconductor, as was done in the earlier nonlinear calculations of GMS and CH. Although this contradicts previous absorption measurements from ZnSe, the calculated dispersion should, in fact, resemble the nonlinear response in GaN since spin-orbit coupling in the latter crystal structure induces negligible valence-band splitting at the absorption edge. We note that the two theoretical approaches determined very similar peak magnitudes to $\chi^{(3)}_{xxxx}$ in ZnSe with slightly different dispersion at photon energies below the ZnSe band edge.

From the comparison in Fig. 3, the $\chi^{(3)}_{xxxx}$ spectra for both materials are resonantly enhanced at the absorption edge, with little contribution from higher interband transitions at this energy. The dispersion in GaN is in good agreement with the results of GMS for photon energies prior to and including the absorption edge; a reasonable correlation to CH is shown in the vicinity of E_g with slightly less agreement below the band edge. The E_1 critical point resonance tends to influence the dispersion in

the E_0 region more strongly in ZnSe, since this optical resonance is much closer to the absorption edge in ZnSe ($E_1 \sim 4.8$ eV) than in the GaN ($E_1 \sim 7$ eV). As such, the $\chi^{(3)}_{xxxx}$ spectrum in GaN does not decrease as rapidly above the absorption edge, due to the weak overlap of these two resonances.

The magnitude of $\chi^{(3)}_{xxxx}$ in GaN is approximately twice as large as the predicted values in ZnSe despite the lower band-gap energy of the latter. The higher ionicity in the II-VI wide-band-gap semiconductors, where electrons are more tightly bound and hence less polarizable than in the III-V systems, may be responsible for the weaker nonlinearity in ZnSe. This behavior is analogous to the ionicity dependence in $\bar{\chi}^{(2)}$, where highly ionic, wide-band-gap semiconductors have much weaker second-order nonlinearities than materials with highly covalent bonds.[24] It is noted that the $\chi^{(3)}_{xxxx}$ calculations of II-VI and III-V semiconductors in CH and GMS also predict larger $\chi^{(3)}_{xxxx}$ values in the latter.

V. CONCLUSIONS

In summary, we have performed a nonlinear TH transmission measurement to determine the dispersion and magnitude of the $\chi^{(3)}_{xxxx}$ nonlinear coefficient in epitaxial wurtzite GaN on sapphire. The response was observed to be enhanced at the fundamental absorption edge, with a peak magnitude of 2.7×10^{-11} esu, with a monotonic decrease for increasing photon energies. The dispersion was found to be consistent with previous band-structure calculations of $\chi^{(3)}_{xxxx}$ in wide-band-gap zinc-blende semiconductors. In particular, the dispersion of $\chi^{(3)}_{xxxx}$ in GaN was very found to be similar to the predicted response in ZnSe.

*Author to whom correspondence should be addressed.

[1]S. R. Marder, L.-T. Cheng, B. G. Tiemann, A. C. Friedli, M. Blanchard-Desce, J. W. Perry, and J. Skindoj, Science **263**, 511 (1994); A. Penxkofer and W. Leupacher, *Organic Materials for Non-Linear Optics* (Royal Society of Chemistry, London, 1989), p. 189.

[2]L. S. Hung, J. A. Agostinelli, J. M. Mir, and L. R. Zheng, Appl. Phys. Lett. **62**, 3071 (1993); J. Agostinelli and G. H. Braunstein, *ibid.* **63**, 123 (1993); A. A. Wernberg, H. J. Gysling, A. J. Filo, and T. N. Blanton, *ibid.* **62**, 946 (1993).

[3]D. J. Moss, E. Ghahramani, J. E. Sipe, and H. M. van Driel, Phys. Rev. B **41**, 1542 (1990); D. J. Moss, E. Ghahramani, and J. E. Sipe, Phys. Status Solidi B **164**, 587 (1991); J. E. Sipe and E. Ghahramani, Phys. Rev. B **48**, 11 705 (1993).

[4]E. Ghahramani, D. J. Moss, and J. E. Sipe, Phys. Rev. B **43**, 9700 (1991).

[5]M. J. Shaw, D. Ninno, B. M. Adderley, and M. Jaros, Phys. Rev. B **45**, 11 031 (1992).

[6]M-Z. Huang and W. Y. Ching, Phys. Rev. B **47**, 9464 (1993).

[7]W. Y. Ching and M.-Z. Huang, Phys. Rev. B **47**, 9479 (1993).

[8]C.C. Wang and E. L. Baardsen, Phys. Rev. **185**, 1079 (1969).

[9]W. K. Burns and N. Bloembergen, Phys. Rev. B **4**, 3437 (1971).

[10]S. Strite and H. Morkoc, J. Vac. Sci. Technol. B **10**, 1238 (1992), and references within.

[11]S. Bloom, J. Phys. Chem. Solids **32**, 2027 (1971); S. Bloom, G. Harbeke, E. Meier, and I. B. Ortenburger, Phys. Status Solidi B **66**, 161 (1974).

[12]Y.-N. Xu and W. Y. Ching, Phys. Rev. B **48**, 4335 (1993); K. Miwa and A. Fukumoto, *ibid.* **48**, 7897 (1993); W. R. L. Lambrecht and B. Segall, in *Wide Band-Gap Semiconductors*, edited by T. D. Moustakas, J. I. Pankove, and Y. Hamakawa, MRS Symposia Proceedings No. 242 (Materials Research Society, Pittsburgh, 1992), p. 367.

[13]J. Miragliotta, D. K. Wickenden, T. J. Kistenmacher, and W. A. Bryden, J. Opt. Soc. Am. B **10**, 1447 (1993).

[14]I. M. Catalano, A. Cingolani, M. Lugara, and A. Minafra, Opt. Commun. **23**, 419 (1977); T. Ishidate, K. Inoue, and M. Aoki, Jpn. J. Appl. Phys. **19**, 1641 (1980).

[15]D. K. Wickenden, T. J. Kistenmacher, W. A. Bryden, J. S. Morgan, and A. Estes-Wickenden, in *Heteroepitaxy of Dissimilar Materials*, edited by R. F. C. Farrow, J. B. Harbison, R. S. Peercy, and A. Zangwill, MRS Symposia Proceedings No. 221 (Materials Research Society, Pittsburgh, 1991), p. 167.

[16]M. D. Levenson, IEEE J. Quantum Electron. **QE-10**, 110 (1974).

[17]J. W. Shelton and Y. R. Shen, Phys. Rev. Lett. **26**, 538 (1971); K. Miyano, T. Nishiwaki, and A. Tomioka, Opt. Commun. **91**, 501 (1992).

[18]Y. R. Shen, *Principles of Nonlinear Optics*, 1st ed. (Wiley, New York, 1984), Chap. 2.

[19]I. H. Malitson, J. Opt. Soc. Am. **52**, 1377 (1967).

[20]R. Boyd, *Nonlinear Optics* (Academic, New York, 1992), Chap. 2.

[21]H. Amano, N. Watanabe, N. Koide, and I. Akasaki, Jpn. J. Appl. Phys. **32**, L1000 (1993).

[22]R. Dingle, D. D. Sell, S. E. Stokowski, and M. Ilegems, Phys. Rev. B **4**, 1211 (1971); B. Moemar, *ibid.* **10**, 676 (1974).

[23]S. Adachi, Phys. Rev. B **43**, 9569 (1991).

[24]B. F. Levine, Phys. Rev. B **7**, 2600 (1973).